JUNE 01 2000

Cell model calculations of dynamic drag parameters in packings of spheres

Olga Umnova; Keith Attenborough; Kai Ming Li

J. Acoust. Soc. Am. 107, 3113–3119 (2000)
https://doi.org/10.1121/1.429340

Cell model calculations of dynamic drag parameters in packings of spheres

Olga Umnova
Department of Environmental and Mechanical Engineering, Faculty of Technology, The Open University, Milton Keynes MK7 6AA, United Kingdom

Keith Attenborough[a)]
School of Engineering, The University of Hull, Hull HU6 7RX, United Kingdom

Kai Ming Li
Department of Mechanical Engineering, Hong Kong Polytechnic University, Kowloon, Hong Kong

(Received 26 October 1998; accepted for publication 16 February 2000)

An external flow approach is used to predict the viscous drag due to oscillating flow in an air-filled stack of fixed identical rigid spheres. Analytical expressions for dynamic and direct current (dc) permeability, high-frequency limit of tortuosity, and the characteristic viscous dimension are derived using a cell model with an adjustable cell radius which allows for hydrodynamic interactions between the spherical particles. The resulting theory requires knowledge of two fixed parameters: the volume porosity and the particle radius. The theory also requires a value for the cell radius. Use of the cell radius corresponding to that of the sphere circumscribing a unit cell of a cubic lattice arrangement is proposed. This is found to enable good agreement between predictions of the new theory and both published data and numerical results for simple cubic and random spherical packings. © *2000 Acoustical Society of America.* [S0001-4966(00)04405-2]

PACS numbers: 43.35.Bf [HEB]

INTRODUCTION

Models for the acoustical properties of porous granular materials may be classified as ''internal'' and ''external'' flow models. Internal flow models (or pore-based models) derive expressions for the viscous force that assumes that the fluid phase exists in tubular pores in the rigid frame. Two recent pore-based models for rigid-framed absorbers[1,2] have been shown to give improved agreement with acoustical data compared with simpler models that assume uniform identical pores. One of them[1] requires information about porosity, tortuosity, flow resistivity, and the pore geometry. The pore geometry is described by two characteristic dimensions. These may be deduced from laboratory measurements, including the Brunauer–Emmett–Teller (BET) method, or approximated from other measured parameters. The other model[2] requires information about the ''pore'' size distribution. This may be obtained through use of laboratory techniques such as water suction or mercury injection for granular materials. These measurements are tedious and time consuming if the ''pores'' are small. The question arises of whether it is possible to derive alternative models for the acoustic behavior of porous granular materials based, for example, on knowledge of the constituent grain sizes and packing characteristics.

External-flow models consider the fluid flow around constituent particles rather than in hypothetical pores. They require knowledge of porosity (or particle volume fraction), particle shape, particle size, and the properties of the packing. The drag force between phases in dilute suspensions is calculated as the sum of the forces between the moving fluid and each particle. In concentrated suspensions and granular materials, there will be interactions between the flows around particles. Cell models such as those by Kuwabara[3] and Happel,[4] modified by Strout,[5] for the oscillatory motion of the fluid have been developed to account for such interactions. In these models, each cell consists of a central particle core and a concentric shell of fluid. The hydrodynamic interactions between particles are taken into account through the boundary conditions on the outer surface of the cell. In the Kuwabara model, the vorticity of fluid velocity is supposed to be zero. In the Happel model the shear stress is assumed zero at the cell boundary. Cell models have been found to give good predictions for the acoustical properties of concentrated suspensions of spherical particles.[5] A cell model, with additional averaging over the distribution of the Voronoi cells, has been applied to calculations of the flow resistivity of fibrous materials.[6] In highly concentrated systems the applicability of the cell model approach becomes questionable. Neighboring solid particles will be in contact and hence will penetrate the hypothetical cell around each individual particle. Nevertheless, in this paper, we will show that adjustment of the cell radius enables reasonable values of DC permeability, tortuosity, and the characteristic viscous dimension of a material consisting of rigidly fixed stacked spheres, even for some types of close packing. In fact, we propose use of a cell radius that has a simple geometrical interpretation.

Section I reinterprets the high- and low-frequency limits of the complex tortuosity function derived by Johnson *et al.*[7] in terms of dynamic drag. In Sec. II these results are compared with the corresponding limits of a modified form of the Kuwabara/Strout cell model. This enables derivation of explicit analytical expressions for the acoustical constants and

a)Author to whom correspondence should be addressed.

the geometrical factor as functions of porosity, particle radius, and cell radius. In Sec. III we find an appropriate expression for cell radius and compare the predictions of the resulting theory with published data and with numerical results obtained independently for different types of packing. Section IV offers concluding remarks.

I. COMPLEX DENSITY, TORTUOSITY, AND PERMEABILITY IN THE EXTERNAL FLOW MODEL

Consider a fluid-filled granular material of porosity ϕ and consisting of rigid identical spherical particles of radius R. Suppose that the solid phase density is much greater than that of the fluid (continuous phase). In this case, the momentum conservation equation for the fluid is

$$\phi\rho_0\frac{\partial v}{\partial t}=-\phi\frac{\partial p}{\partial x}-D(\omega)v, \tag{1}$$

where ρ_0 is the fluid density, p is the pressure variation in the sound wave, v is the fluid velocity averaged over unit volume of the fluid, and $D(\omega)$ is the frequency-dependent drag coefficient.

The waves are supposed to be harmonic and, consequently, $\partial/\partial t\rightarrow -i\omega$.

The complex density of the fluid is defined by

$$\rho(\omega)=-\frac{\partial p}{\partial x}\frac{1}{-i\omega v}=\rho_0\left(1+\frac{D(\omega)}{-i\omega\rho_0\phi}\right). \tag{2a}$$

The complex density in a rigid-framed porous material is related to the complex tortuosity $\alpha(\omega)$ and complex permeability $k(\omega)$ defined by Johnson,[7]

$$\begin{aligned}\alpha(\omega)&=\frac{\rho(\omega)}{\rho_0},\\ k(\omega)&=\frac{i\eta\phi}{\omega\rho(\omega)}=\frac{i\eta\phi}{\omega\rho_0(1+(-D(\omega)/i\omega\rho_0\phi))}.\end{aligned} \tag{2b}$$

Johnson[7] has considered the analytical properties of the linear response function $\alpha(\omega)$ as well as its low- and high-frequency limits viz.,

$$\begin{aligned}\lim_{\omega\rightarrow 0}\alpha(\omega)&=\frac{\phi}{k_0}\frac{i\eta}{\omega\rho_0},\\ \lim_{\omega\rightarrow\infty}\alpha(\omega)&=\alpha_\infty+\left(\frac{i\eta}{\omega\rho_0}\right)^{1/2}\frac{2\alpha_\infty}{\Lambda},\end{aligned} \tag{3}$$

where α_∞ is the high-frequency limit of tortuosity (known simply as tortuosity in many publications; for example, see Ref. 2), k_0 is the DC permeability, and Λ is the characteristic viscous dimension of the material.

From (3) and (2), the following limits for the drag term can be obtained:

$$\lim_{\omega\rightarrow 0}D(\omega)=\frac{\phi^2\eta}{k_0}, \tag{4a}$$

$$\lim_{\omega\rightarrow\infty}D(\omega)=-i\omega\rho_0\phi\left[(\alpha_\infty-1)+\left(\frac{i\eta}{\omega\rho_0}\right)^{1/2}\frac{2\alpha_\infty}{\Lambda}\right]. \tag{4b}$$

II. THE DRAG FORCE IN THE PRESENCE OF HYDRODYNAMIC INTERACTIONS BETWEEN RIGID PARTICLES

Consider the oscillatory flow of incompressible viscous fluid with macroscopic velocity $\mathbf{v}e^{-i\omega t}$ around a fixed spherical particle. The fluid velocity field around a sphere can be represented by[8]

$$\mathbf{u}=[\mathbf{v}+\mathrm{curlcurl}(f(r)\mathbf{v})]e^{-i\omega t},$$

where $f(r)$ is the potential function.

The components of the fluid velocity in a polar coordinate system (with the polar axis z parallel to $\mathbf{v}$) are

$$u_\theta=-v\ \sin\ \theta\left(1-\frac{df}{rdr}-\frac{d^2f}{dr^2}\right),$$

$$u_r=v\ \cos\ \theta\left(1-2\frac{df}{rdr}\right).$$

The potential function obeys the following equation:

$$\frac{d}{dr}\left(\Delta\Delta f-\frac{\omega\rho_0}{i\eta}\Delta f\right)=0, \tag{5}$$

where $\Delta=d^2/dr^2+(2/r)d/dr$ is the radial part of the spherical Laplacian operator.

The nonslip boundary conditions ($u_\vartheta|_R=u_r|_R=0$, where R is the particle radius) are applied on the particle surface. In terms of the potential function they can be rewritten as

$$\left.\frac{df}{rdr}\right|_R=\frac{1}{2}, \tag{6}$$

$$\Delta f|_R=\tfrac{3}{2}. \tag{7}$$

In the Kuwabara/Strout model[3,5] the vorticity of the fluid velocity is assumed to be zero at the outer cell boundary ($\mathrm{curl}\ \mathbf{u}|_b=0$, where b is the cell radius). In terms of the potential function that means that

$$\left.\frac{d\Delta f}{dr}\right|_b=0. \tag{8}$$

In the original version of the Strout/Kuwabara model, the radial component of fluid velocity is assumed to vanish at the external cell boundary. Instead, we choose the value that results from matching the magnitude of the macroscopic fluid velocity v with the z component of the fluid particle velocity averaged over the cell volume. Hence

$$\begin{aligned}\langle u_z\rangle_v&=\frac{2\pi}{\frac{4}{3}\pi(b^3-R^3)}\int_0^\pi\int_R^b(u_r(r,\theta)\cos\ \theta\\ &\quad-u_\theta(r,\theta)\sin\ \theta)r^2\ \sin\ \theta d\theta dr\\ &=v-\frac{2v}{b^3-R^3}\left(b^2\left.\frac{df}{dr}\right|_b-\frac{R^3}{2}\right)=v.\end{aligned}$$

It should be noted that the nonslip boundary condition (6) has been used here. From this equation, the boundary condi-

tion for the radial component of the fluid velocity on the outer cell boundary can be obtained. In terms of potential function it has the form

$$\left.\frac{df}{rdr}\right|_b = \frac{\Theta}{2}, \tag{9}$$

where

$$\Theta = \left(\frac{R}{b}\right)^3. \tag{10}$$

The magnitude of the drag force, F, parallel to the direction of the velocity, v, is calculated from[8]

$$F = \int (-P\cos\theta + \sigma_{rr}\cos\theta - \sigma_{r\theta}\sin\theta)df,$$

where the integration is performed over the spherical particle surface.

The components of the stress tensor are

$$\sigma_{rr} = 2\eta\frac{\partial u_r}{\partial r}, \quad \sigma_{r\theta} = \eta\left(\frac{\partial u_r}{r\partial\theta} + \frac{\partial u_\theta}{\partial r} - \frac{u_\theta}{r}\right).$$

The pressure P on the particle surface is calculated from the equations of fluid motion in the polar coordinate system and is connected with the potential function in the following way:

$$P = P_0 + \eta v R\cos\theta \times\left(\left.\frac{d\Delta f}{rdr}\right|_R - \Delta\Delta f|_R - \left(\frac{\omega\rho_0}{i\eta}\right)\left(\left.\frac{df}{rdr}\right|_R - \Delta f|_R\right)\right).$$

Using boundary conditions (6), (7) the expression for the drag force becomes

$$F = \frac{4}{3}\pi R^3 v\,\eta\left(-3\left.\frac{d\Delta f}{rdr}\right|_R + \Delta\Delta f|_R - \frac{\omega\rho_0}{i\eta}\right).$$

The drag term is calculated as the sum of the drag forces on individual particles,

$$D(\omega) = \frac{nF}{v}, \tag{11}$$

where $n = (1-\phi)/(4/3)\pi R^3$ is the number of particles per unit volume.

As a result of solving Eq. (5) with boundary conditions (6)–(9), we get

$$D(\omega) = +i\omega\rho_0(1-\phi)\left(1 + \frac{3}{2}(\Theta^{-1}-1) \times\frac{\exp(2s(\Theta^{-1/3}-1))A_1 + A_2}{\exp(2s(\Theta^{-1/3}-1))B_1 - B_2}\right), \tag{12}$$

where

$$A_1 = (s\Theta^{-1/3}-1)(s^2+3s+3),$$

$$A_2 = (s\Theta^{-1/3}+1)(s^2-3s+3),$$

$$B_1 = (s\Theta^{-1/3}-1)(-s^2(\Theta^{-1}-1)+3s+3),$$

$$B_2 = (s\Theta^{-1/3}+1)(s^2(\Theta^{-1}-1)+3s-3),$$

and $s = \sqrt{(\omega\rho_0/i\eta)R^2}$.

The high-frequency limit of the drag term is

$$D(\omega\to\infty) \to -i\omega\rho_0(1-\phi)\left[\frac{1}{2} + \frac{9}{2(1-\Theta)R}\left(\frac{i\eta}{\omega\rho_0}\right)^{1/2}\right].$$

Comparison of this expression with (4b) yields explicit expressions for the high-frequency limit of tortuosity and the characteristic viscous dimension in terms of porosity, grain radius, and cell radius,

$$\Lambda = \frac{4(1-\Theta)\phi\alpha_\infty}{9(1-\phi)}R, \tag{13}$$

$$\alpha_\infty = 1 + \frac{1-\phi}{2\phi}. \tag{14}$$

The latter expression coincides with the well-known result for tortuosity obtained by Berryman[9] and is independent of the cell radius.

Comparison of the low-frequency limit of $D(\omega)$, i.e.,

$$D(\omega\to 0) \to \frac{9\eta(1-\Theta)(1-\phi)\Omega_k}{2R^2},$$

with (4a) gives an explicit expression for dc permeability,

$$k_0 = \frac{2}{9}\frac{\phi^2}{(1-\phi)(1-\Theta)\Omega_k}R^2, \tag{15}$$

where

$$\Omega_k = \frac{5}{5 - 9\Theta^{1/3} + 5\Theta - \Theta^2} \tag{16}$$

is Kuwabara's low-frequency correction factor.

These results for Λ, α_∞, and k_0 are exact to first nontrivial order in solid concentration $1-\phi$.

Our modification of the boundary condition for the radial component of fluid velocity does not change the expression for k_0 and Λ that would have resulted from use of the original version of Strout/Kuwabara theory. However, it changes the predicted value of tortuosity significantly. The assumption of zero r-component of velocity at the outer cell boundary gives

$$\alpha_\infty = 1 + \frac{(1-\phi)}{2\phi}(1+2\Theta). \tag{14'}$$

This expression leads to values of tortuosity that exceed the results of numerical calculations and data by a significant margin.

The geometrical factor is defined by

$$M = \frac{8\alpha_\infty k_0}{\Lambda^2\phi}, \tag{17}$$

and corresponds to $2n^2/s$ in the notation of Attenborough,[10] where n is the dynamic shape factor and s is the static shape factor. For materials with cylindrical pores

$$\alpha_\infty = \frac{1}{\cos^2\theta}, \quad k_0 = \frac{1}{8}\phi a^2\cos^2\theta, \quad \Lambda = a,$$

where a is the pore radius and θ is the angle between the pores and the sound propagation direction. Hence the geo-

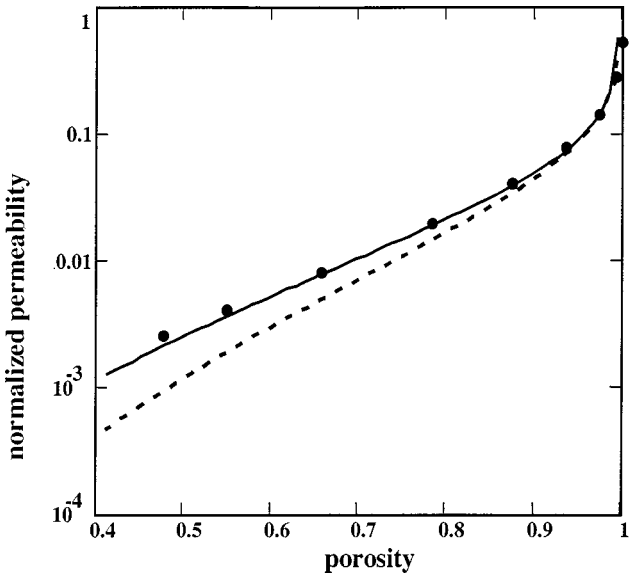

FIG. 1. Dimensionless dc permeability k_0/d^2 [$d=\sqrt[3]{(4\pi)/(3(1-\phi))}R$ is the base vector of the lattice] for SC packing as a function of porosity, circles—numerical results (Ref. 12), solid line—cell model (19), dashed lines—cell model (18).

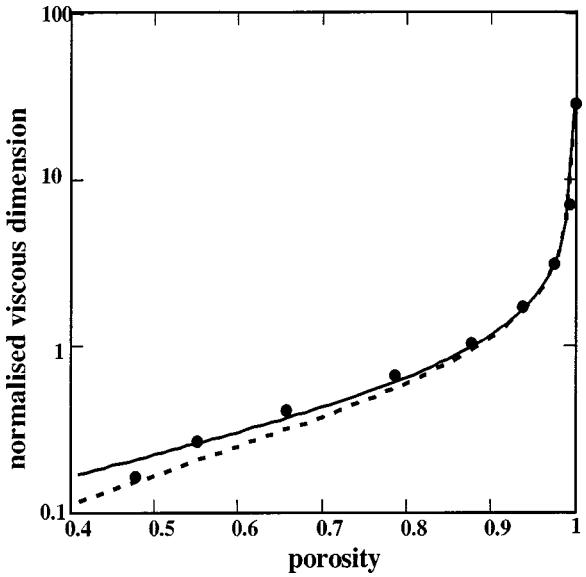

FIG. 2. Dimensionless characteristic viscous dimension Λ/d for SC packing as a function of porosity, circles—numerical results (Ref. 12) for SC packing, solid line—cell model (19) results, dashed lines—cell model (18) results.

metrical factor is 1 for a material with cylindrical pores. Allard[1] suggests that M could take values up to 10 for materials with noncylindrical pores. On the other hand, Johnson[7] has found that $M=1$ gives the best agreement between his predictions and data for glass beads. Numerical simulations with an intersecting tubes model[11] indicate that M is approximately constant (i.e., changes within a factor of two) over the range of porosity that causes k_0 to vary over eight orders of magnitude.

III. COMPARISONS WITH NUMERICAL RESULTS AND DATA

So far we have not defined the parameter Θ—the ratio of the particle volume to the cell volume. In the original version of the Kuwabara/Strout model it was taken to be equal to the volume fraction of the solid phase in the material,

$$\Theta=1-\phi. \tag{18}$$

Instead, we propose use of larger spherical cells based on spheres that circumscribe the unit cells of the packing. In this case for simple cubic (SC) packing,

$$\Theta=\frac{3}{\sqrt{2}\pi}(1-\phi)\cong 0.675(1-\phi), \tag{19}$$

Chapman and Higdon have calculated the drag parameters and the dynamic permeability of different packings of identical spherical particles numerically.[12]

In Fig. 1, their numerical predictions of DC permeability for SC packing for the range of porosities up to the close packing limit $\phi_c=0.4764$ are compared with cell model results. If the model with modified cell radius (19) is used, there is tolerable agreement (within 18%) even at a porosity corresponding to close packing. With the unmodified cell radius (18), the agreement with numerical results is good only for very dilute systems. In Fig. 2 the corresponding comparisons for characteristic viscous dimension are presented. The results of cell model with modified radius are closer to numerical values than those with the unmodified radius, except for close packing. Overall, the error is not more than 20% for the modified cell model, whereas with the unmodified theory and some values of porosity, it exceeds 40%.

In fact, our choice (19) of the connection between porosity and the parameter Θ in SC packing corresponds to the minimum of the mean value of the absolute difference between numerical results[12] and cell model estimates. With the cell radius given by $\Theta/(1-\phi)=0.675$, then, for DC permeability,

$$\varepsilon_k=\frac{1}{N}\sum_{i=1}^{N}\frac{|k_0^{\text{num}}-k_0^{\text{cell}}|}{k_0^{\text{num}}}\times 100\%=5.8\%,$$

where N is the number of points with different porosity where comparisons are made. Similarly with $\Theta/(1-\phi)=0.675$, then, for characteristic viscous dimension,

$$\varepsilon_\Lambda=\frac{1}{N}\sum_{i=1}^{N}\frac{|\Lambda^{\text{num}}-\Lambda^{\text{cell}}|}{\Lambda^{\text{num}}}\times 100\%=7.3\%.$$

If $\Theta/(1-\phi)=0.6$, then $\varepsilon_k\cong 8.2\%$ and $\varepsilon_\Lambda=10.7\%$, if $\Theta/(1-\phi)=0.8$ then $\varepsilon_k=11.5\%$ and $\varepsilon_\Lambda=10.7\%$.

In Fig. 3, the cell model predictions of formation factor $F=\alpha_\infty/\phi$ are compared with numerical results. Since the value of formation factor does not depend on parameter Θ in the cell model, both versions give the same results. The deviation between the numerical results and the cell model estimates does not exceed 12% even for close packing. Figure 4 shows that modified cell model predictions for magnitude and phase of dynamic permeability $k(\omega)$ are also in reasonable agreement with numerical results[12] for SC packing.

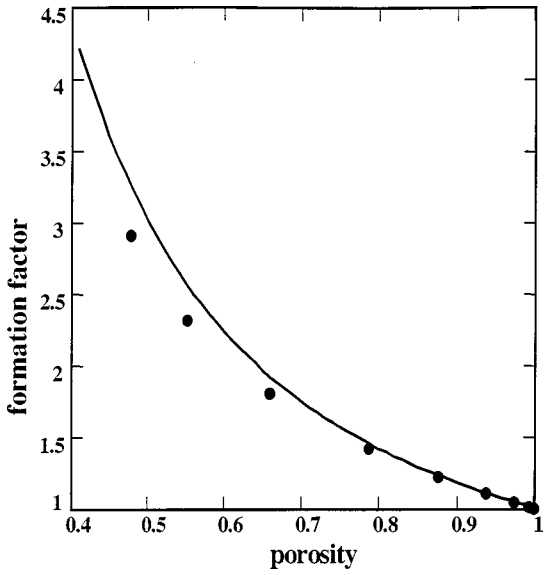

FIG. 3. Formation factor $F=\alpha_\infty/\phi$ as a function of porosity, circles—numerical results (Ref. 12) for SC packing, solid line—cell model results.

Nevertheless, the results indicate that the cell model is not sufficiently accurate to reproduce the differences between the various forms of packing obtained numerically. Moreover, the modified cell model results differ significantly from the numerical estimates for close packings. This indicates that the cell model is not able to describe such dense systems.

Wong *et al.*[16] have presented data for the formation factor and dc permeability of fused glass beads with porosities between 0.023 and 0.399. For the highest porosity $\phi=0.399$, the measured value of formation factor is close to 4. For this value of porosity, the modified cell model predicts $F=4.375$. The measured value for dc permeability is approximately 3×10^{-12} m^2 for a mixture of glass beads with diameters between 44×10^{-6} and 53×10^{-6} m. The modified cell model predicts 1.95×10^{-12} m$^2\leqslant k_0\leqslant 2.83\times10^{-12}$ m^2, where the first figure corresponds to smaller particles.

For a mixture of beads with diameters between 88×10^{-6} and 106×10^{-6} m, the measured value of DC permeability is approximately 10^{-11} m^2, and the modified cell model predicts $7.79\times10^{-12}\,\mathrm{m}^2\leqslant k_0\leqslant 11.31\times10^{-12}\,\mathrm{m}^2$.

Predictions of the cell model [with parameter Θ calculated using either (18) or (19)] are compared with data[13–15] for permeability, tortuosity, and characteristic viscous dimension of random packings of bronze spheres and glass beads in Tables I and II. The number of nearest neighbors in close random packing is similar to that in (6) in simple cubic packing, so we use expression (19) to connect cell radius with porosity in random packing also. The predictions of the theory with modified cell radius agree well with two series of data.[13,14] However, there are discrepancies between predictions and the data for high-frequency constants of two data sets [Ref. 13, series 3 and Ref. 15]. Neither the original nor modified cell models give predictions that match these data in most cases. On the other hand, it is noticeable that the geometrical factors for these data have unusually large values. Moreover there is a significant difference between these data and those for tortuosity and characteristic viscous di-

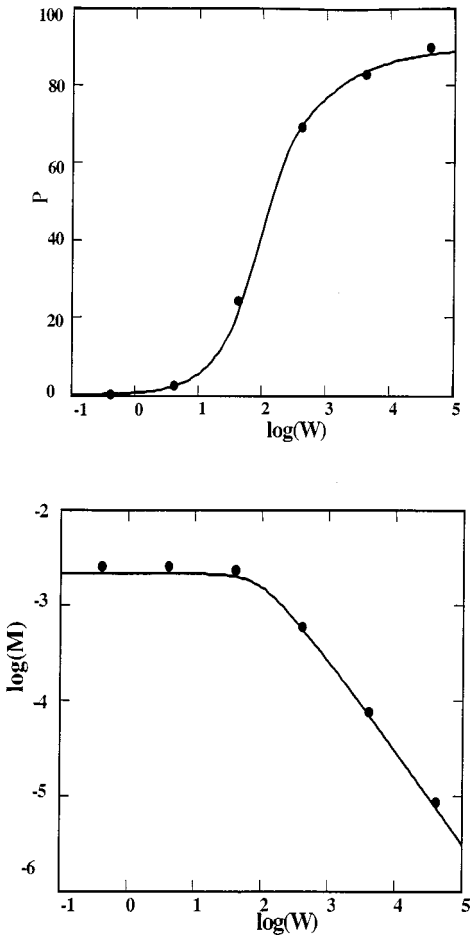

FIG. 4. Phase $\tan^{-1}(\mathrm{Im}(k(\omega))/\mathrm{Re}(k(\omega)))$, in degrees, and magnitude $M(\omega)=|k(\omega)/d^2|$ of dynamic permeability as a function of dimensionless frequency $W=(\omega\rho_0 d^2/\eta)$ for SC lattice. Circles—numerical results (Ref. 12), solid line—cell model (19) results.

TABLE I. Comparison of cell model predictions and data for dc permeability, tortuosity, characteristic viscous dimension, and geometrical parameter in packings of bronze spheres. (Brackets indicate parameter values deduced from those of the others.)

Parameters	k_0 (mm^2)	α_∞	Λ (mm)	M	
$\phi=0.43$ $R=0.0375$ mm	$7*10^{-6}$	(1.61)	$1.24*10^{-2}$	1.34	Bronze spheres data series 1[a]
	$7.57*10^{-6}$	1.66	$1.29*10^{-2}$	1.42	Cell model (19) prediction
	$2.97*10^{-6}$	1.66	$0.90*10^{-2}$	1.14	Cell model (18) prediction
$\phi=0.41$ $R=0.055$ mm	$12.00*10^{-6}$	(1.97)	$1.79*10^{-2}$	1.44	Bronze spheres data series 2[a]
	$13.40*10^{-6}$	1.72	$1.76*10^{-2}$	1.74	Cell model (19) prediction
	$5.00*10^{-6}$	1.72	$1.2*10^{-2}$	1.4	Cell model (18) prediction
$\phi=0.41$ $R=0.25$ mm	$1.90*10^{-4}$	(2.70)	$5.32*10^{-2}$	3.54	Bronze spheres data series 3[a]
	$2.77*10^{-4}$	1.72	$7.99*10^{-2}$	1.74	Cell model (19) prediction
	$1.03*10^{-4}$	1.72	$5.44*10^{-2}$	1.4	Cell model (18) prediction

[a]See Ref. 13.

TABLE II. Comparison of cell model predictions and data for dc permeability, tortuosity, characteristic viscous dimension, and geometrical parameter in packings of glass beads.

Parameters	k_0 (mm^2)	α_∞	Λ (mm)	M	
$\phi=0.5$ $R=0.85$ mm	$8.0*10^{-3}$	1.42	$4.40*10^{-1}$	1.0	Fused glass bead data series 1[a]
	$7.45*10^{-3}$	1.50	$3.75*10^{-1}$	1.26	Cell model (19) prediction
	$3.43*10^{-3}$	1.50	$2.83*10^{-1}$	1.02	Cell model (18) prediction
$\phi=0.5$ $R=0.475$ mm	$1.83*10^{-3}$	1.56	$2.18*10^{-1}$	1.02	Fused glass bead data series 2[a]
	$2.33*10^{-3}$	1.50	$2.10*10^{-1}$	1.26	Cell model (19) prediction
	$1.07*10^{-3}$	1.50	$1.58*10^{-1}$	1.02	Cell model (18) prediction
$\phi=0.5$ $R=0.25$ mm	$0.44*10^{-3}$	1.49	$1.10*10^{-1}$	1.02	Fused glass bead data series 3[a]
	$0.64*10^{-3}$	1.50	$1.10*10^{-1}$	1.26	Cell model (19) prediction
	$0.30*10^{-3}$	1.50	$0.83*10^{-1}$	1.02	Cell model (18) prediction
$\phi=0.4$ $R=0.73$ mm	$1.51*10^{-3}$	1.37	$0.90*10^{-1}$	5.1	Stacked glass beads data[b]
	$2.15*10^{-3}$	1.75	$2.25*10^{-1}$	1.48	Cell model (19) prediction
	$0.76*10^{-3}$	1.75	$1.51*10^{-1}$	0.8	Cell model (18) prediction

[a]See Ref. 14.
[b]See Ref. 15.

mension obtained with materials having similar values for the radius and volume fraction of particles.

The frequency dependencies of predicted and measured[14] values of the real and the imaginary parts of the scaled dynamic permeability $k(\omega)/k_0$ in a random packing are presented in Fig. 5.

However, cell model estimates of DC permeability are significantly lower than numerical results.[17,18] For example, for close SC packing, the numerical result[17] is $k_0/R^2\phi = 2.065\times10^{-2}$, whereas the modified cell model predicts $k_0/R^2\phi = 1.14\times10^{-2}$.

Calculation of formation factor for close SC packing using (14′) and (19) gives $F=4.068$. This exceeds both the numerical result[12] $F=2.906$ and the modified cell model prediction $F=3.253$. For data series 2,[14] (14′) and (19) give $\alpha_\infty=1.838$. Again this value exceeds both the measured value $\alpha_\infty=1.56$ and the modified cell model result $\alpha_\infty=1.5$.

IV. CONCLUDING REMARKS

The Kuwabara/Strout cell model has been modified to match the macroscopic and the cell-volume averaged velocities and by increasing the cell volume. Analytical expressions for acoustical/drag parameters have been obtained in terms of three parameters: the volume fraction of the solid phase, the particle radius, and the cell radius. If the cell radius is defined by that of the sphere that circumscribes a unit cell in a cubic lattice, then the values of drag parameters predicted by the new cell model are in good agreement with numerical results[12] for simple cubic packing and measured

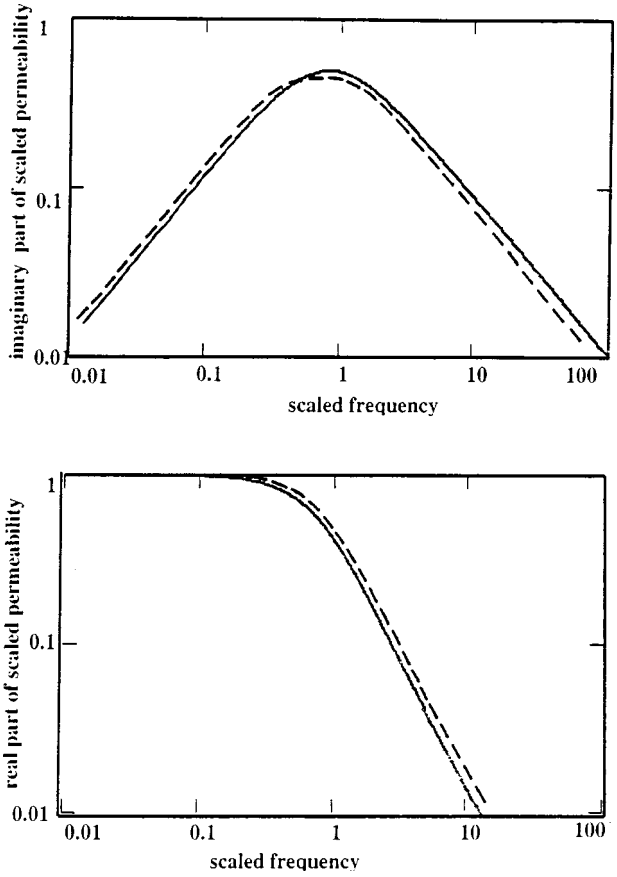

FIG. 5. Real and imaginary parts of the scaled dynamic permeability $k(\omega)/k_0$ as a function of the scaled frequency ω/ω_c [$\omega_c = \eta(1-\phi)/\rho_0\alpha_\infty k_0$]. The solid line represents cell model predictions and the broken line corresponds to fused glass bead data (Ref. 14) series 1–3.

data for sintered bronze spheres and fused glass beads.[13,14,16] This is encouraging for our ultimate aim of using the cell model approach for deducing the acoustical properties of granular materials. Further publications will be concerned with new similarity relationships between viscous and thermal characteristics and with the calculation of bulk acoustical parameters.

ACKNOWLEDGMENT

The work was supported by EPSRC (U.K.) through Grant No. GR/L61804.

[1] J-F. Allard, *Propagation of Sound in Porous Media* (Elsevier Science, Essex, U.K., 1993).
[2] K. Attenborough, ''Models for acoustical properties of air-saturated granular media,'' Acta Acust. **1**, 213–226 (1993).
[3] S. Kuwabara, ''The forces experienced by randomly distributed parallel circular cylinders or spheres in a viscous flow at small Reynolds numbers,'' J. Phys. Soc. Jpn. **14**, 527–532 (1959).
[4] J. Happel, ''Viscosity of suspensions of uniform spheres,'' J. Appl. Phys. **28**, 1288–1292 (1957).
[5] T. A. Strout, ''Attenuation of sound in high concentration suspensions: Development and application of an oscillatory cell model,'' Ph.D. Thesis, University of Maine, 1991.
[6] V. Tarnow, ''Calculation of the dynamic air flow resistivity of fiber materials,'' J. Acoust. Soc. Am. **102**, 1680–1688 (1997).
[7] D. L. Johnson, J. Koplik, and R. Dashen, ''Theory of dynamic permeabil-

ity and tortuosity in fluid-saturated porous media,'' J. Fluid Mech. **176**, 379–402 (1987).
[8] L. D. Landau and E. M. Lifshitz, *Fluid Mechanics* (Butterworth–Heineman, Oxford, 1987).
[9] J. G. Berryman, ''Confirmation of Biot's theory,'' Appl. Phys. Lett. **37**, 382–384 (1980).
[10] K. Attenborough, ''Acoustical characteristics of rigid porous absorbents and granular materials,'' J. Acoust. Soc. Am. **73**, 785–799 (1983).
[11] D. L. Johnson, J. Koplik, and L. M. Schwartz, ''New pore-size parameter characterizing transport in porous media,'' Phys. Rev. Lett. **57**, 2564–2567 (1986).
[12] A. M. Chapman and J. J. L. Higdon, ''Oscillatory Stokes flow in periodic porous media,'' Phys. Fluids A **4**, 2099–2116 (1992).
[13] S. R. Baker and I. Rudnick, ''Measurement of the Biot structural factor-sigma for sintered bronze spheres,'' IEEE Trans. Antennas Propag. **33**, 118 (1986); *Proceedings of the 1985 IEEE Ultrasonic Symposium*, San Francisco, 1985 (IEEE, New York, 1986).
[14] E. Charlaix, A. P. Kushnick, and J. P. Stokes, ''Experimental study of dynamic permeability in porous media,'' Phys. Rev. Lett. **61**, 1595–1598 (1988).
[15] J. F. Allard, M. Henry, J. Tizianel, L. Kelders, and W. Lauriks, ''Sound propagation in air saturated random packings of beads: Surface waves over bead layers,'' J. Acoust. Soc. Am. **104**, 2004–2007 (1998).
[16] P.-Z. Wong, J. Koplik, and J. P. Tomanic, ''Conductivity and permeability of rocks,'' Phys. Rev. B **30**, 6606–6614 (1984).
[17] M.-Y. Zhou and P. Sheng, ''First-principle calculations of dynamic permeability in porous media,'' Phys. Rev. B **39**, 12027–12039 (1989).
[18] A. S. Sangani and A. Acrivos, ''Slow flow through a periodic array of spheres,'' Int. J. Multiphase Flow **8**, 343–360 (1982).